Effect of Particle Nonsphericity on Bidirectional Reflectance of Cirrus Clouds

M. I. Mishchenko, W. B. Rossow, A. Macke, and A. A. Lacis
National Aeronautics and Space Administration
Goddard Institute for Space Studies
New York, New York

Previous analyses of the First International Satellite Cloud Climatology Project (ISCCP) Regional Experiment (FIRE) measurements have been interpreted as indicative of asymmetry parameters of the cirrus cloud particle phase function on the order of 0.75 or smaller (Wielicki et al. 1990; Kinne et al. 1994). Ray tracing computations for single or aggregated hexagonal ice crystals cannot produce such small asymmetry parameters (Takano and Liou 1989; Macke 1994). Furthermore, there is accumulating evidence that the idealized phase function associated with regular hexagonal particles and exhibiting pronounced halos is not representative of the reflectance characteristics of the majority of cirrus clouds (Minnis et al. 1993; Sassen et al. 1994; Wielicki et al. 1990; Francis 1995). On the other hand, ray tracing computations of the phase function for irregular fractal ice particles (Macke 1994) show no halo features and can have asymmetry parameters approaching 0.75. Therefore, in this paper we use the fractal ice particle model to study the differences in bidirectional reflectance caused by the differences in the single scattering phase functions of spherical water droplets and nonspherical ice crystals.

The solid line in Figure 1 shows the phase function for randomly oriented, irregular, fractal particles with shape depicted in the insert. The size-parameter-independent scattering component of the phase function was computed using the ray-tracing method (Macke 1994), while the size-parameter-dependent diffraction component was averaged over a size distribution with an effective radius r_{eff} = 30 μm. Remarkably, this phase function not only shows no pronounced halo features, but also has an asymmetry parameter as small as 0.752. For comparison, the dotted line shows the phase function for the water cloud particle model (gamma distribution of spherical droplets with an effective radius r_{eff} = 10 μm) used in the ISCCP (Rossow et al. 1991).

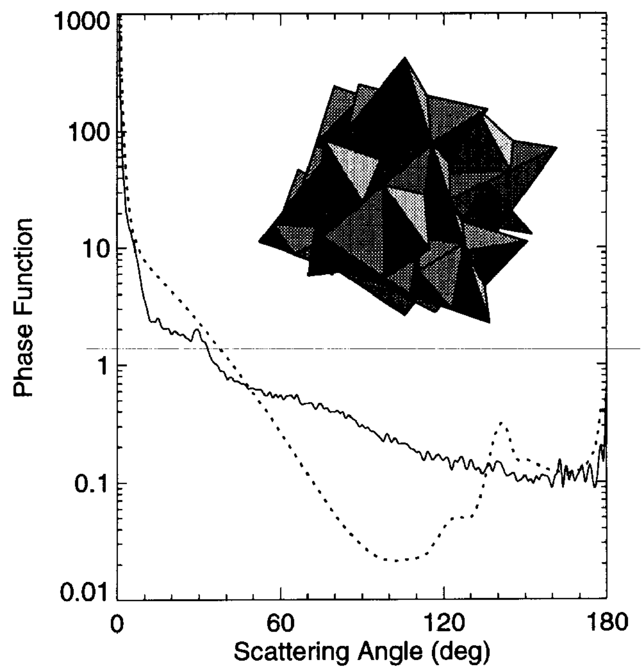

Figure 1. Phase functions of fractal ice particles (solid line) and ISCCP water droplets (dotted line) at 0.63 μm.

We have used the two phase functions in accurate multiple scattering calculations for plane-parallel water and ice clouds with varying optical thickness. Bidirectional cloud reflectivity was computed using the standard adding/doubling method (Hansen and Travis 1974) without introducing any further approximations like the truncation of the forward-scattering peak of the phase function. The number of Gaussian quadrature points in zenith angle discretization and the number of terms in the Fourier decomposition of the reflection function were increased until the relative accuracy of computing the reflection function was better than 10^{-3}.

Figure 2 shows the ratio $\varrho(\tau_i)$ of the reflectivity computed for the ice cloud with optical thicknesses τ_i = 0.3, 0.1, 3, and 300 relative to that of the liquid water cloud with optical thickness τ_w = 1. Cosines of the sun, μ_0, and satellite, μ, zenith angles vary from 0.2 to 1, and relative satellite-sun azimuth angles are φ = 0, 90, and 180°.

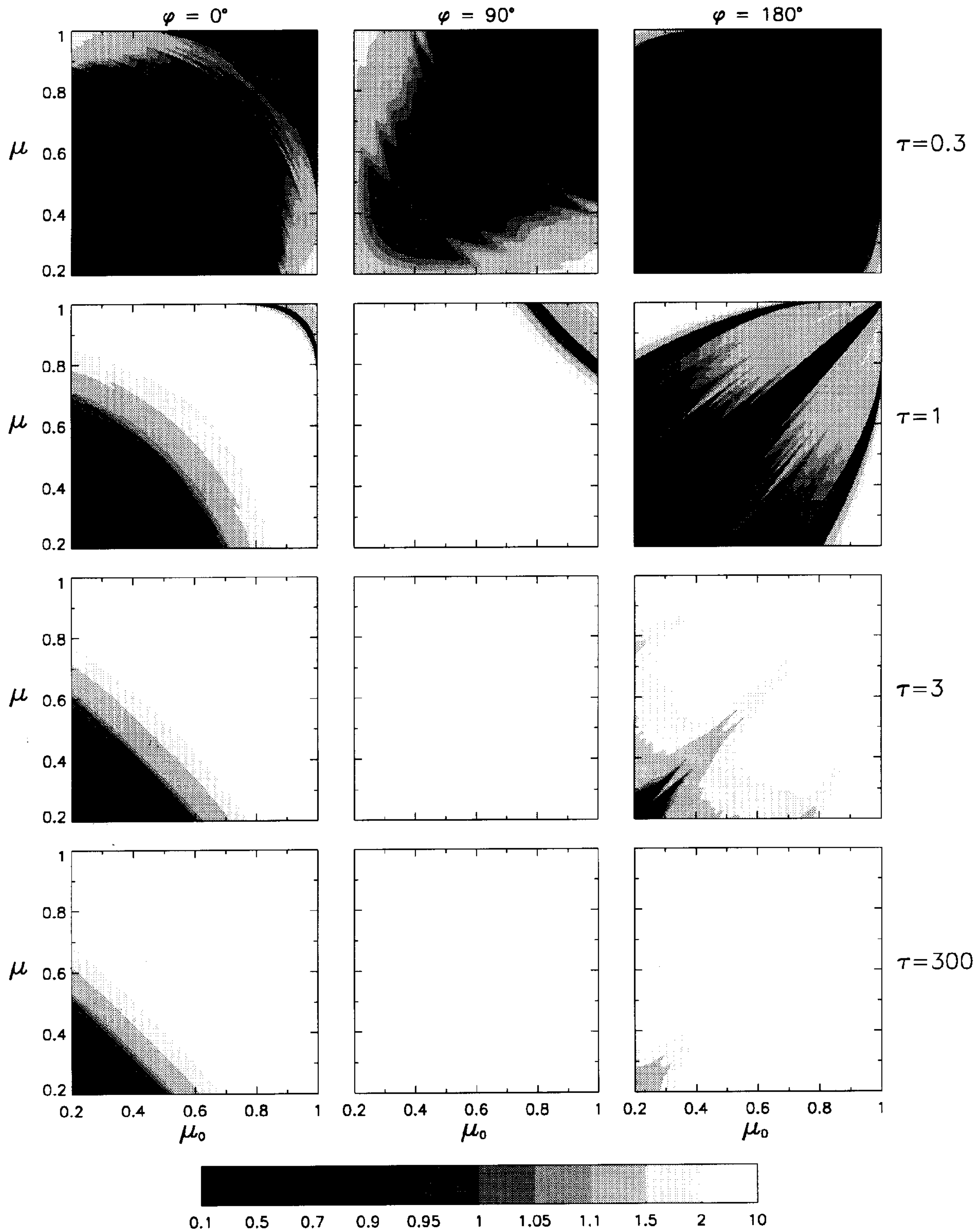

Figure 2. Ratio $\varrho(\tau_i)$ of the reflectivity computed for the ice cloud with optical thicknesses τ = 0.3, 0.1, 3, and 300 relative to that of the liquid water cloud with optical thickness τ_w = 1. Solid lines show contours at the level ϱ = 1.

Computations for $\tau_i = 1$ show that nonspherical/spherical differences in reflectance exactly follow those in the single-scattering phase functions (Figure 1). Specifically, the ice cloud reflectivity is larger at side-scattering angles and smaller at near-forward- and back-scattering angles. Furthermore, the large single-scattering differences cause values of ϱ larger than two for $\tau_i \ll \tau_w$ and values of ϱ smaller than 0.5 for $\tau_i \gg \tau_w$. Remarkably, at $\varphi = 0$ and μ and μ_0 smaller than about 0.5, the reflectivity of the water cloud with $\tau_w = 1$ cannot be reproduced by the ice cloud with optical thickness as large as 300. Our computations show that the region of $\varrho < 1$ at $\varphi = 0$ and small μ and μ_0 survives even if the ice cloud is semi-infinite. This means that at near-forward-scattering geometries water clouds with optical thickness of order one can produce reflectivities that cannot be matched by ice clouds with an arbitrarily large optical thickness.

Figure 2 can be used to examine the errors in the retrieved cloud optical thickness introduced by the use of the wrong cloud particle model. Specifically, the contours at the level $\varrho = 1$ indicate the retrieved optical thickness as a function of μ, μ_0, and φ if the ice cloud model is used to analyze reflectance measurements for a liquid water cloud with optical thickness $\tau_w = 1$. Figure 2 shows that the retrieved optical thickness is strongly scattering-geometry-dependent and can substantially differ from the actual value 1 (Mishchenko et al. 1995). Following the differences in the single-scattering phase functions (Figure 1), the ice cloud model overestimates the retrieved optical thickness at near-forward- and back-scattering geometries and underestimates it at side-scattering geometries. The errors in the retrieved optical thickness are especially large at near-forward-scattering geometries (i.e., at $\varphi = 0$ and small μ and μ_0). Furthermore, at μ and μ_0 smaller than 0.5, the retrieval scheme using the ice particle model produces no solution at all.

References

Francis, P. N. 1995. Some aircraft observations of the scattering properties of ice crystals, *J. Atmos. Sci.*, **52**, 1142-1154.

Hansen, J. E., and L. D. Travis. 1974. Light scattering in planetary atmospheres, *Space Sci. Rev.*, **16**, 527-610.

Kinne, S., R. Bergstrom, T. P. Ackerman, A. J. Heymsfield, J. DeLuisi, M. Shiobara, P. Pilewskie, F.P.J. Valero, and Y. Takano. 1994. Cirrus cloud solar radiative properties: Comparisons between theory and observations based measurements during FIRE'91. In *8th Conference on Atmospheric Radiation*, American Meteorological Society, Boston, pp. 238-240.

Macke, A. 1994. Modeling of the optical properties of cirrus clouds, Ph. D. Thesis, University of Hamburg.

Minnis, P., P. W. Heck, and D. F. Young. 1993. Inference of cirrus cloud properties using satellite-observed visible and infrared radiances. II: Verification of theoretical cirrus radiative properties, *J. Atmos. Sci.*, **50**, 1305-1322.

Mishchenko, M. I., A. A. Lacis, B. E. Carlson, and L. D. Travis. 1995. Nonsphericity of dust-like tropospheric aerosols: Implications for aerosol remote sensing and climate modeling, *Geophys. Res. Lett.*, **22**, 1077-1080.

Rossow, W. B., L. C. Garder, P.-J. Lu, and A. W. Walker. 1991. *International Satellite Cloud Climatology Project (ISCCP) Documentation of Cloud Data*, WMO/TD, No. 266 (Revised), World Climate Research Programme (ICSU and WMO), Geneva.

Sassen, K., N. C. Knight, Y. Takano, and A. J. Heymsfield. 1994. Effects of ice-crystal structure on halo formation: Cirrus cloud experimental and ray-tracing modeling studies, *Appl. Opt.*, **33**, 4590-4601.

Takano, Y., and K. N. Liou. 1989. Solar radiative transfer in cirrus clouds. 1. Single-scattering and optical properties of hexagonal ice crystals, *J. Atmos. Sci.*, **46**, 3-19.

Wielicki, B. A., J. T. Suttles, A. J. Heymsfield, R. M. Welch, J. D. Spinherne, M. L. Wu, D. O'C. Starr, L. Parker, and R. F. Ardvini. 1990. The 27-28 October 1986 FIRE IFO Cirrus Case Study: Comparison of radiative transfer theory with observations by satellite and aircraft, *Mon. Wea. Rev.*, **118**, 2356-2376.